This article was downloaded by: [Duke University Libraries]
On: 15 January 2013, At: 12:24
Publisher: Taylor & Francis
Informa Ltd Registered in England and Wales Registered Number: 1072954
Registered office: Mortimer House, 37-41 Mortimer Street, London W1T 3JH, UK

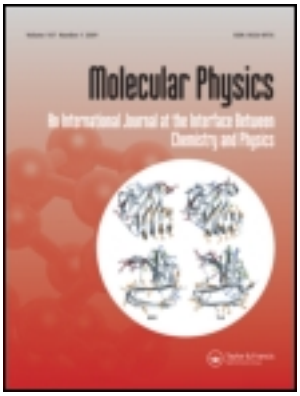

Molecular Physics: An International Journal at the Interface Between Chemistry and Physics

Publication details, including instructions for authors and subscription information:
http://www.tandfonline.com/loi/tmph20

Reactive canonical Monte Carlo

J. Karl Johnson [a] , Athanassios Z. Panagiotopoulos [b] & Keith E. Gubbins [b]

[a] Complex Systems Theory Branch, Naval Research Laboratory, Washington, D.C., 20375-5345, USA

[b] School of Chemical Engineering, Cornell University, Ithaca, NY, 14853, USA

Version of record first published: 22 Aug 2006.

To cite this article: J. Karl Johnson , Athanassios Z. Panagiotopoulos & Keith E. Gubbins (1994): Reactive canonical Monte Carlo, Molecular Physics: An International Journal at the Interface Between Chemistry and Physics, 81:3, 717-733

To link to this article: http://dx.doi.org/10.1080/00268979400100481

PLEASE SCROLL DOWN FOR ARTICLE

Full terms and conditions of use: http://www.tandfonline.com/page/terms-and-conditions

This article may be used for research, teaching, and private study purposes. Any substantial or systematic reproduction, redistribution, reselling, loan, sub-licensing, systematic supply, or distribution in any form to anyone is expressly forbidden.

The publisher does not give any warranty express or implied or make any representation that the contents will be complete or accurate or up to date. The accuracy of any instructions, formulae, and drug doses should be independently verified with primary sources. The publisher shall not be liable for any loss, actions, claims, proceedings, demand, or costs or damages whatsoever or howsoever caused arising directly or indirectly in connection with or arising out of the use of this material.

MOLECULAR PHYSICS, 1994, VOL. 81, NO. 3, 717–733

Reactive canonical Monte Carlo
A new simulation technique for reacting or associating fluids

By J. KARL JOHNSON
Complex Systems Theory Branch, Naval Research Laboratory,
Washington, D.C. 20375-5345, USA

ATHANASSIOS Z. PANAGIOTOPOULOS and KEITH E. GUBBINS
School of Chemical Engineering, Cornell University, Ithaca, NY 14853, USA

(*Received 9 June 1993; accepted 20 August 1993*)

A new simulation technique is developed for calculating the properties of chemically reactive and associating (hydrogen bonding, charge transfer) systems. We call this new method reactive canonical Monte Carlo (RCMC). In contrast to previous methods for treating chemical reactions, this algorithm is applicable to reactions involving a change in mole number. Stoichiometrically balanced reactions are attempted in the forward and reverse directions to achieve chemical equilibrium. The transition probabilities do not depend on the chemical potentials or chemical potential differences of any of the components. We also extend RCMC to work in concert with the isothermal–isobaric ensemble for simulating chemical reactions at constant pressure, and with the Gibbs ensemble for simultaneous calculation of phase and chemical equilibria. Association is treated as a chemical reaction in the RCMC formalism. Results are presented for dimerization of simple model associating fluids. In contrast to previous methods, the reactive Gibbs ensemble can be used to calculate phase equilibrium for associating fluids with very strong bonding sites. RCMC simulations are performed for nitric oxide dimerization and results are compared with available experimental data in the liquid phase. Agreement with experiment is excellent. Results for a vapour phase simulation are also in remarkable agreement with estimates based on second virial coefficient data.

Downloaded by [Duke University Libraries] at 12:24 15 January 2013

1. Introduction

Reliable methods for predicting the thermodynamics of associating fluids (e.g. water, alcohols, amines) are needed in many chemical and biological applications. Recently there has been much interest in developing statistical mechanical theories of molecular association and in performing computer simulations as a means of testing the theories [1–12]. In a previous paper [12] we presented computer simulations for phase equilibria of associating fluids with moderately strong bonding sites, $\epsilon^{\text{bond}}/\epsilon^{\text{LJ}} \approx 10$, where ϵ^{bond} and ϵ^{LJ} are the well depths for the bonding (association) and Lennard-Jones (LJ) interactions, respectively; for stronger bonding sites equilibration was prohibitively slow using conventional simulation methods. The models with moderate bonding strengths studied previously show appreciable association in the liquid phase at low temperatures, but little bonding near the critical point or in the vapour phase. Many real associating fluids exhibit greater bonding, and more vapour phase association than shown by our previous models. In order to solve the problem of simulating strongly associating fluids, we have developed a new

0026-8976/94 $10.00 © 1994 Taylor & Francis Ltd.

simulation ensemble that facilitates direct sampling of the formation and destruction of bonds in the fluid. We treat association as a chemical reaction; the new simulation technique can be used to study chemical reaction equilibrium as well as physical association. We call our method reactive canonical Monte Carlo (RCMC).

In our previous work we modelled association by using a simple pair potential comprised of a reference term ϕ^{ref}, and a bonding term ϕ^{bond},

$$\phi(12) = \phi^{\text{ref}}(12) + \sum_A \sum_B \phi_{AB}^{\text{bond}}(r_{AB}), \tag{1}$$

where (12) stands for the positions and orientations of molecules 1 and 2, ϕ_{AB}^{bond} is the attractive potential between association sites A and B on molecules 1 and 2, r_{AB} is the site–site distance between site A on molecule 1 and site B on molecule 2, and the summations are over all bonding sites. We used the LJ 6–12 potential for ϕ^{ref}, and square-well attractive sites for ϕ_{AB}^{bond}. For off-centre spherical square-well bonding sites the bonding potential is written as

$$\phi_{AB}^{\text{bond}}(r_{AB}) = \begin{cases} -\epsilon^{\text{bond}}, & \text{if } r_{AB} < \sigma_b, \\ 0, & \text{if } r_{AB} > \sigma_b, \end{cases} \tag{2}$$

where ϵ^{bond} is the depth of the square-well and σ_b is the diameter of the square-well bonding site. The bonding site is located a distance l_b from the centre of the reference LJ sphere.

Methods that have previously been developed to simulate chemically reactive systems [13–17] have all been confined to reactions that conserve the number of molecules, and so are not applicable to association reactions such as dimerization, etc. Coker and Watts [13] used a modification of the grand canonical Monte Carlo (GCMC) technique to calculate chemical equilibrium. Their method requires the specification of the chemical potential difference between any two species. The method of Kofke and Glandt [14] involves a modification of GCMC they call the semi-grand canonical ensemble. In the semi-grand ensemble the chemical potential differences between all the species and a reference species are specified. This method has been extended to the isobaric ensemble, and an extension to the Gibbs ensemble [18, 19] has been outlined, but not implemented [14]. Sindzingre *et al.* [15, 16] developed a simulation method also based on chemical potential differences. Shaw [17] developed a new isobaric Monte Carlo simulation method based on the atomic rather than the molecular viewpoint. Shaw's method is called the $N_{\text{atoms}}PT$ ensemble, and does not involve specifying the chemical potential differences. Our method is more similar in spirit to Shaw's than to the other methods cited.

2. Derivation of reactive canonical Monte Carlo

The grand canonical partition function for a mixture of C components is

$$\Xi = \sum_{N_1=0}^{\infty} \cdots \sum_{N_C=0}^{\infty} Q(N_1, \ldots, N_C, V, T) \exp\left(\beta \sum_{i=1}^{C} N_i \mu_i\right), \tag{3}$$

where N_i is the number of molecules of type i, V is the volume of the system, $\beta = 1/kT$, T is the temperature, k is Boltzmann's constant, $Q(\cdots)$ is the canonical

Downloaded by [Duke University Libraries] at 12:24 15 January 2013

partition function for the mixture and μ_i is the chemical potential for component i in the mixture. If we approximate Q semi-classically then we obtain [20]

$$\Xi = \sum_{N_1=0}^{\infty} \cdots \sum_{N_C=0}^{\infty} \int \cdots \int \exp\left[\beta \sum_{i=1}^{C} N_i \mu_i - \sum_{i=1}^{C} \ln(N_i!) + \sum_{i=1}^{C} N_i \ln(q_i) - \beta \mathscr{U}\right] \mathrm{d}\mathbf{s}^{N_1} \, \mathrm{d}\omega^{N_1} \cdots \mathrm{d}\mathbf{s}^{N_C} \, \mathrm{d}\omega^{N_C}, \tag{4}$$

where $\mathbf{s} = \mathbf{r}/V^{1/3}$ is a set of scaled position coordinates [21] $\mathbf{s}^{N_i} \equiv \mathbf{s}_1 \cdots \mathbf{s}_{N_i}$, and $\omega^{N_i} \equiv \omega_1 \cdots \omega_{N_i}$ are the orientations of the N_i molecules of type i, q_i is the partition function for an isolated molecule of type i and $\mathscr{U}$ is the configurational energy of the mixture. To a good approximation, the q_is for molecules can be written as a product of translational and internal contributions [20]

$$q_i = q_{i,t} q_{i,r} q_{i,v} q_{i,e}, \tag{5}$$

where $q_{i,t} = V/\Lambda^3$ is the translational partition function, with Λ the de Broglie wavelength, and $q_{i,r}$, $q_{i,v}$ and $q_{i,e}$ are the rotational, vibrational and electronic partition functions, respectively. Now consider a chemical reaction involving any number of the species in the mixture. This may be written as [22]

$$\sum_{i=1}^{C} \nu_i M_i = 0, \tag{6}$$

where M_i is the chemical symbol for component i and ν_i is the stoichiometric coefficient of component i (positive for products, negative for reactants, and zero for species that do not enter the reaction). For any chemical reaction at equilibrium we may write

$$\sum_{i=1}^{C} \nu_i \mu_i = 0. \tag{7}$$

There is no need to specify the reaction at this point; the development is for any single reaction. Borrowing notation from Shaw [17], we denote as r an arbitrary initial state of the system $(\mathbf{s}^{N_1} \omega^{N_1} \cdots \mathbf{s}^{N_C} \omega^{N_C})$. The probability that a system will be in state r is

$$P_r = \frac{1}{\Xi} \exp\left[\beta \sum_{i=1}^{C} N_i \mu_i - \sum_{i=1}^{C} \ln(N_i!) + \sum_{i=1}^{C} N_i \ln(q_i) - \beta \mathscr{U}_r\right], \tag{8}$$

where $\mathscr{U}_r$ is the configurational energy of state r. If a single reaction proceeds in the forward direction from state r to a new state s then the probability of observing that state is

$$P_s = \frac{1}{\Xi} \exp\left[\beta \sum_{i=1}^{C} \nu_i \mu_i + \beta \sum_{i=1}^{C} N_i \mu_i - \sum_{i=1}^{C} \ln[(N_i + \nu_i)!] + \sum_{i=1}^{C} \nu_i \ln(q_i) + \sum_{i=1}^{C} N_i \ln(q_i) - \beta \mathscr{U}_s\right]. \tag{9}$$

Taking the ratio $P_s/P_r = P_{r \to s}$ gives the transition probability for a single reaction in

Downloaded by [Duke University Libraries] at 12:24 15 January 2013

the forward direction. If we assume chemical equilibrium we obtain

$$P_{r\to s} = \exp\left\{\sum_{i=1}^{C} \ln\left[\frac{N_i!}{(N_i+\nu_i)!}\right] + \sum_{i=1}^{C} \nu_i \ln(q_i) - \beta\delta\mathscr{U}_{r\to s}\right\}, \tag{10}$$

where $\delta\mathscr{U}_{r\to s} = \mathscr{U}_s - \mathscr{U}_r$. The chemical potentials have dropped out of equation (10) by application of equation (7). Equation (10) can be re-written as

$$P_{r\to s} = \exp(-\beta\delta\mathscr{U}_{r\to s}) \prod_{i=1}^{C} q_i^{\nu_i} \prod_{i=1}^{C} \frac{N_i!}{(N_i+\nu_i)!}. \tag{11}$$

We note that the term $\Pi_{i=1}^{C} q_i^{\nu_i}$ is related to the ideal gas equilibrium constant defined by Hill [23],

$$K^{id}(T) = \prod_{i=1}^{C} (q_i/V)^{\nu_i} = \frac{\prod_{i=1}^{C} q_i^{\nu_i}}{\prod_{i=1}^{C} V^{\nu_i}}, \tag{12}$$

where V is the volume of the system.

Now consider a single reaction in the reverse direction with the final state labelled as t. The transition probability for a reaction in the reverse direction, $P_{r\to t}$, can be generated simply by replacing ν_i by $-\nu_i$ in equation (11).

Neither the chemical potentials nor the chemical potential differences appear in equation (11). For a single reaction in a two component mixture the Gibbs phase rule states that there are two degrees of freedom to specify. We may therefore choose to specify the temperature, and either the density or the pressure of the system. The first choice corresponds to the RC NVT ensemble, and the second corresponds to the RC NPT ensemble, where N stands for the number of atoms, rather than the number of molecules. In contrast, the pressure cannot be specified in a GCMC simulation because this would over-specify the system.

3. Results for $2A \rightleftharpoons B$

The development so far has been general, without specifying the reaction. Now let us consider the specific reaction of monomers associating to form dimers (e.g. nitric oxide or acetic acid dimerization), or equivalently, a chemical reaction such as atomic hydrogen forming H_2. This can be written in general as a chemical reaction

$$2A \rightleftharpoons B, \tag{13}$$

where A is a monomer molecule and B is a dimer molecule. Applying equation (11) to this reaction gives

$$P_{r\to s} = \exp(-\beta\delta\mathscr{U}_{r\to s}) \frac{(N_A)(N_A-1)q_B}{(N_B+1)q_A^2}, \tag{14}$$

for the forward reaction. The reverse reaction is given by

$$P_{r\to t} = \exp(-\beta\delta\mathscr{U}_{r\to t}) \frac{N_B q_A^2}{(N_A+2)(N_A+1)q_B}. \tag{15}$$

The extension to reactions involving three chemical species $(A + B \rightleftharpoons C)$ is

Downloaded by [Duke University Libraries] at 12:24 15 January 2013

straightforward. We present here an algorithm for performing a simulation using RCMC for the $2A \rightleftharpoons B$ reaction. We choose a move at random with fixed probability from the list below and iterate to equilibrate and collect averages:

(1) Choose a molecule at random and attempt a change in position and orientation.
(2) If the pressure is held constant attempt a random change in the volume.
(3) Attempt a forward reaction step.
    (*a*) Choose a molecule of type A at random.
    (*b*) Change that molecule to type B, picking a random orientation.
    (*c*) Choose another molecule of type A at random and delete it from the fluid.
    (*d*) Accept the move with a probability of min $[1, P_{r\rightarrow s}]$.
(4) Attempt a reverse reaction step.
    (*a*) Choose a molecule of type B at random.
    (*b*) Change that molecule to type A.
    (*c*) Randomly insert a molecule of type A into the fluid.
    (*d*) Accept the move with a probability of min $[1, P_{r\rightarrow t}]$.

Note that moves 3 and 4 must be chosen with equal probability in order to ensure microscopic reversibility. Note also that only monomers need to be inserted at random into the fluid. Dimers are inserted into the cavity created by the deletion of a monomer, so this method avoids the problem associated with inserting a chain into a dense fluid. This is also true for higher mers, for example with $A + A_2 \rightleftharpoons A_3$ trimers would be inserted into a dimer cavity, and in the reverse reaction only a monomer would be inserted. Because we are inserting a monomer into the fluid, the RCMC method will fail at high densities where Widom's particle insertion method [24] will also fail. For the special case of mole-conserving reactions, (e.g. $A + B \rightleftharpoons 2C$) the algorithm reduces to one similar to that of Shaw [17]. However, unlike Shaw's algorithm RCMC is also valid for reactions that involve a change in the number of moles.

We have tested the RCMC algorithm for the $2A \rightleftharpoons B$ reaction by comparing with results from GCMC simulations for mixtures. We initially used a very simple model for a reacting fluid that only required the specification of the dissociation energy, D_0 and the equilibrium bond length, r_e to specify the intra-dimer potential. The monomers (A) are LJ spheres and the dimers (B) are two-site LJ diatomics with the site–site parameters chosen to be the same as those for the A molecules. To calculate the partition functions in equations (14) and (15) for molecules A and B we have assumed the following: molecule A is monatomic and so q_A consists only of translational partition function

$$q_t = \left(\frac{2\pi mkT}{h^2}\right)^{3/2} V, \tag{16}$$

where m is the mass of the molecule, h is Planck's constant and V is the volume of the system. Molecule B is by definition a homonuclear diatomic, and so has internal degrees of freedom. We assume that B is a rigid molecule with a fixed bond length r_e. This gives a rotational partition function of

$$q_r = \frac{2\pi^2 m r_e^2 kT}{h^2}, \tag{17}$$

Downloaded by [Duke University Libraries] at 12:24 15 January 2013

which includes the symmetry number of 2. The translational contribution for B is given by equation (16) with m replaced by $2m$. We also consider the vibrational and electronic partition functions (assuming that the nuclear contribution is unity). If we allow only ground state electronic contributions with no degeneracy, and take the zero of energy as two separated monomers at rest, we can write

$$q_v q_e = \frac{\exp(\beta D_0)}{1 - \exp(-\beta h\nu)}, \tag{18}$$

where D_0 is the dissociation energy and ν is the vibrational frequency. For convenience we have chosen $\beta h\nu \gg 1$ so that we may replace $1 - \exp(-\beta h\nu)$ by unity.

We have performed both GCMC and RCMC simulations on the model presented above and the results are reported in the table. For these simulations we have chosen $D_0 = 15\epsilon^{LJ}$ and the mass and LJ parameters for methane: $m = 16{\cdot}04\,\mathrm{g\,mol^{-1}}$, $\epsilon^{LJ}/k = 149{\cdot}1\,\mathrm{K}$ and $\sigma = 3{\cdot}743\,\text{Å}$. We have chosen the diatomic bond length as $r_e = \sigma$. These choices are completely arbitrary. Because we are using rigid diatomic molecules the details of the intramolecular potential do not need to be specified. The intramolecular partition functions are completely specified by D_0 and r_e. When performing GCMC simulations the chemical potentials of A and B were specified. In order to ensure chemical equilibrium we specified $\mu_B = 2\mu_A$, and then picked μ_A as the independent variable. Both type A and B molecules were created and destroyed independently during the course of a GCMC run. The GCMC simulations gave the thermodynamic properties as a function of $\mu_A^* = \mu_A/\epsilon^{LJ}$ and $T^* = kT/\epsilon^{LJ}$, where ϵ^{LJ} is the LJ well depth. We report reduced densities $\rho^* = N/V\sigma^3$, mole fractions X_A reduced pressures $P^* = P\sigma^3/\epsilon^{LJ}$ and reduced configurational energies $U^* = U/(N\epsilon^{LJ})$ in the table. The average atomic density, $\rho_a^* = (X_A + 2X_B)\rho^*$, collected from the GCMC run was used as the constant atomic density in the reactive canonical (RC) NVT simulations. The independent variables for the RCMC simulations were T^* and ρ_a^*. It is interesting to note that there is apparently a phase change at $T^* = 1{\cdot}6$ between $\mu_A^* = -36$ and $\mu_A^* = -37$. The agreement between the GCMC and RCMC runs is excellent. The GCMC

Table. A comparison of data from GCMC and RCMC simulations for the reaction $2A \rightleftharpoons B$ where A is a LJ atom and B is a LJ diatomic (see text). The numbers in parentheses are one standard deviation uncertainties in the last digits of the reported values.

Program	T^*	μ_A^*	ρ^*	X_A	U^*	P^*
GCMC	1·6	−36	0·348(5)	0·083(6)	−7·70(15)	0·48(7)
RCMC	1·6	—	0·3481(9)	0·085(5)	−7·69(3)	0·46(5)
GCMC	1·6	−37	0·0241(1)	0·331(1)	−0·519(7)	0·0327(2)
RCMC	1·6	—	0·02408(1)	0·3302(9)	−0·514(5)	0·0328(2)
GCMC	2·0	−40	0·414(3)	0·179(9)	−7·96(6)	2·61(11)
RCMC	2·0	—	0·414(1)	0·176(6)	−7·97(3)	2·58(8)
GCMC	2·0	−42	0·359(3)	0·20(1)	−6·80(12)	0·92(20)
RCMC	2·0	—	0·3594(7)	0·200(4)	−6·799(25)	1·12(5)
GCMC	2·0	−43	0·307(4)	0·231(12)	−5·60(15)	0·55(4)
RCMC	2·0	—	0·3068(7)	0·231(4)	−5·59(2)	0·541(31)
GCMC	2·0	−44	0·1048(23)	0·401(4)	−1·69(5)	0·147(3)
RCMC	2·0	—	0·1048(1)	0·3992(6)	−1·70(1)	0·149(2)

Downloaded by [Duke University Libraries] at 12:24 15 January 2013

simulations were equilibrated for around 2×10^6 configurations followed by about 6×10^6 configurations for collecting averages (1 configuration = 1 move of any type). The average number of atoms in the simulation cell ranged from about 200 to 500 depending on the state point. For the RCMC simulations the number of atoms was 500 and averages were collected for 10^6 configurations, which followed 10^6 equilibration moves. In both cases the LJ potential was cut off at 3σ and the standard long-range corrections were applied.

The isothermal–isobaric reactive canonical (RC *NPT*) ensemble code has been tested by comparison with RC *NVT* simulations for the fluid described above. The results from these two simulations agree everywhere within the error bars of the simulations. Both the RC *NVT* and RC *NPT* codes have been tested to ensure that they are insensitive to the starting densities and mole fractions.

In the above development we have used a simple model for an associating fluid. We now apply RCMC to fluids with one spherical square-well bonding site as described by equations (1) and (2) and in [12], where ϕ^{ref} is again taken to be the LJ potential. In doing so we must calculate the partition functions corresponding to the given intermolecular and intramolecular potentials. The monomer molecules (type *A*) are monatomic and q_A is given by equation (16). Type *B* molecules are homonuclear diatomics, but they cannot be treated as rigid rotors or harmonic oscillators as in equations (17, 18). In order to find q_B we use classical statistical mechanics to write [23]

$$q_B = \frac{1}{2h^6} \int \mathrm{d}\mathbf{p}_1 \int \mathrm{d}\mathbf{q}_1 \int \mathrm{d}\mathbf{p}_2 \int \mathrm{d}\mathbf{q}_2 \exp\left[-\beta \mathscr{H}(\mathbf{q}_1, \mathbf{q}_2, \mathbf{p}_1, \mathbf{p}_2)\right], \tag{19}$$

where the **p**s and **q**s are the generalized momenta and position coordinates of molecules 1 and 2, which make up a bonded dimer, and $\mathscr{H}$ is the Hamiltonian for the dimer. The factor of 1/2 appears because molecules 1 and 2 are indistinguishable. The integrations are restricted to the ranges for which the dimer is bonded. The Hamiltonian can be written as

$$\mathscr{H} = \frac{\mathbf{p}_1}{2m} + \frac{\mathbf{p}_2}{2m} + U(r_{12}), \tag{20}$$

where m is the mass of a monomer and $U(r_{12})$ is the intramolecular potential. $U(r_{12})$ depends only on the separation of the two monomers, provided that they are bonded, and is given by

$$U(r_{12}) = \phi(r_{12}) - \epsilon^{\text{bond}}, \tag{21}$$

where $\phi(r_{12})$ is the LJ potential. There are no restrictions on the values of the momenta, and the integrations can be easily performed to give

$$q_B = \frac{(2\pi mkT)^3}{2h^6} \int \mathrm{d}\mathbf{q}_1 \int \mathrm{d}\mathbf{q}_2 \exp\left[-\beta U(r_{12})\right]. \tag{22}$$

We now change from generalized position coordinates to atomic separation r_{12} and account for the bonding orientations at a given separation. This has been solved analytically [5] for the bonding model of equation (2). The result is

$$q_B = \frac{(2\pi mkT)^3}{2h^6} 4\pi \int_{2l_b-\sigma_b}^{2l_b+\sigma_b} \frac{(\sigma_b + 2l_b - r_{12})^2 (2\sigma_b - 2l_b + r_{12})}{24 l_b^2} \exp\left[-\beta U(r_{12})\right] r_{12}\, \mathrm{d}r_{12}. \tag{23}$$

Downloaded by [Duke University Libraries] at 12:24 15 January 2013

The integral in equation (23) must be performed numerically for the desired values of σ_b, l_b, ϵ^{bond} and T.

The bonded dimers interacting through the potential of equations (1) and (2) have a variable bond length. The RCMC simulations of this fluid must therefore include Monte Carlo moves in the bond length. The new bond length must be chosen randomly from a non-uniform distribution $P(r_{12})$ which describes the distribution of possible bond lengths. For the square-well model used here $P(r_{12})$ is given by

$$P(r_{12}) = \begin{cases} 0, & \text{if } r_{12} < 2l_b - \sigma_b \\ (\sigma_b + 2l_b - r_{12})^2(2\sigma_b - 2l_b + r_{12})/(r_{12}I), & \text{if } 2l_b - \sigma_b < r_{12} < 2l_b + \sigma_b, \\ 0, & \text{if } r_{12} > 2l_b + \sigma_b \end{cases} \tag{24}$$

where r_{12} is the bond length and I is the normalization integral given by

$$I = \int_{2l_b-\sigma_b}^{2l_b+\sigma_b} \frac{(\sigma_b + 2l_b - r_{12})^2(2\sigma_b - 2l_b + r_{12})}{r_{12}} \, dr_{12}. \tag{25}$$

$P(r_{12})$ is determined solely by the geometry of the bonding site.

The RCMC simulations converge much faster than conventional Monte Carlo (MC) simulations for fluids with strong bonding sites. We have used the same square-well geometric parameters used by Walsh *et al.* [25], $l_b = 0{\cdot}4\sigma$ and $\sigma_b = 0{\cdot}2\sigma$. For an associating fluid with $\epsilon^{\text{bond}} = 20\epsilon^{\text{LJ}}$ at $T^* = 1$ the fraction of monomers in a conventional NVT MC simulation failed to converge after more than 3×10^7 configurations. The fraction of monomers in a RCMC simulation for this same system converged in about 4×10^5 configurations. We have compared RCMC simulations with conventional NVT simulations at higher temperatures where the NVT simulations of the square-well associating fluid converged in a reasonable amount of cpu time. The results are presented in figure 1. Both the fraction of monomers and the internal energies are calculated on an atomic basis. Both NVT and RCMC simulations were performed with 256 atoms. The NVT simulations were equilibrated for about 10^7 configurations, followed by an additional 10^7 configurations for data taking. The RCMC simulations were equilibrated for 10^6 configurations, followed by 10^6 to 2×10^6 data taking

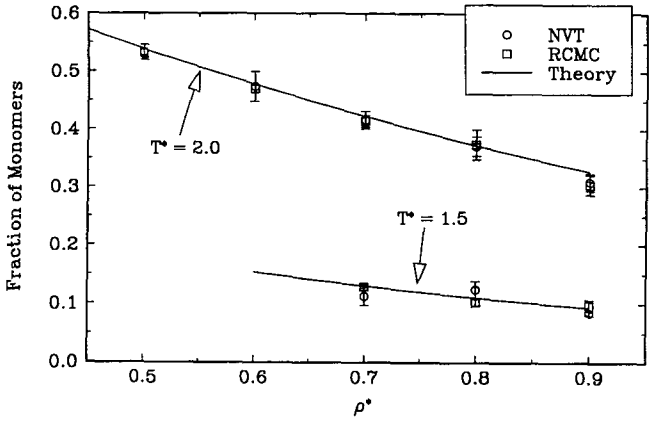

Figure 1. Comparison of RCMC and conventional NVT simulations for the LJ + SW bonding fluid with one bonding site. The bonding site parameters are $\epsilon^{\text{bond}} = 20\epsilon^{\text{LJ}}$, $l_b = 0{\cdot}4\sigma$ and $\sigma_b = 0{\cdot}2\sigma$. The lines are calculations from Wertheim's theory [1–7].

Downloaded by [Duke University Libraries] at 12:24 15 January 2013

configurations. The RCMC reaction moves are computationally more expensive than the simple displacement/reorientation moves. However, in our experience the RCMC technique is typically about five times faster than conventional MC in terms of cpu time. Results from the two simulation techniques agree within the uncertainties of the simulations. Calculations from our implementation [12] of a theory of association due to Wertheim [1–7] are also plotted in figure 1; results from both RCMC and *NVT* simulations agree well with predictions from the theory.

4. Extension to the Gibbs ensemble

The reactive canonical ensemble can be combined with Gibbs ensemble MC [18, 19] to allow simultaneous calculation of phase and chemical equilibria. It is important to note that only one species of the mixture needs to be transferred between boxes. Equality of the chemical potentials of the other species will be achieved by the chemical reaction steps. We are free to choose which species to transfer between the boxes; a judicious choice is the monomer species, thus avoiding transferring larger, polyatomic molecules between the boxes. For the reaction considered above, $2A \rightleftharpoons B$, the pressure cannot be specified in advance because to do so would violate the Gibbs phase rule. Introduction of a third component into the system would provide one more degree of freedom, and the simulations could then be carried out in a constant pressure reactive Gibbs ensemble.

The reactive Gibbs ensemble technique has been used to calculate the vapour–liquid equilibrium properties of a model associating fluid with one square-well bonding site. In figure 2 we show the saturation densities for a fluid with $\epsilon^{\text{bond}} = 10\epsilon^{\text{LJ}}$ from the theory, conventional Gibbs ensemble simulations and from reactive Gibbs ensemble simulations. The conventional and reactive Gibbs simulations agree very well for this system, and both agree well with the Wertheim theory. We show the fraction of monomers for the saturated phases in figure 3. We note that this is a weakly associating fluid, with the vapour phase consisting of almost all monomers. Agreement between the conventional and reactive Gibbs simulations demonstrates that the reactive Gibbs method is reliable for calculating the phase equilibrium properties of the LJ + square-well fluid.

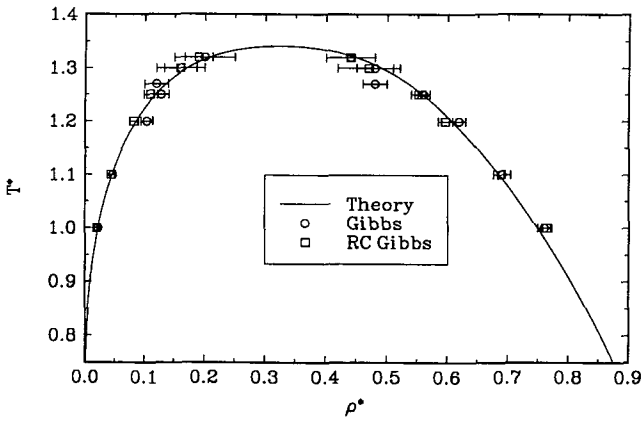

Figure 2. Saturation densities from conventional and reactive Gibbs ensemble simulations for a fluid with one square-well bonding site with $\epsilon^{\text{bond}} = 10\epsilon^{\text{LJ}}$. The line is calculated from the Wertheim theory.

Downloaded by [Duke University Libraries] at 12:24 15 January 2013

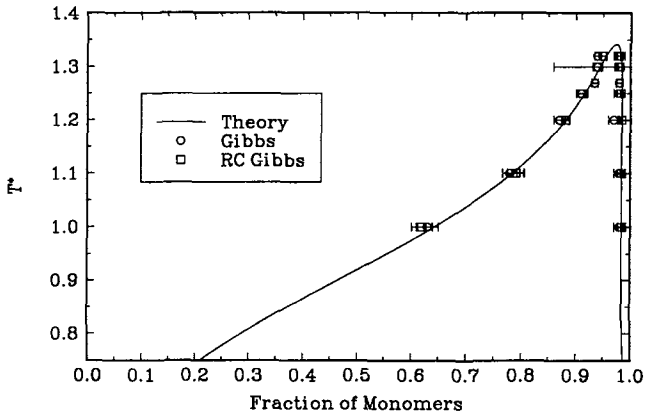

Figure 3. Fraction of monomers from conventional and reactive Gibbs ensemble simulations for a fluid with one square-well bonding site with $\epsilon^{bond} = 10\epsilon^{LJ}$. The line is calculated from the theory.

We have also used the reactive Gibbs ensemble method to simulate a strongly associating fluid with one square-well site and a well depth of $\epsilon^{bond} = 20\epsilon^{LJ}$. The results for the saturation densities and fraction of monomers are shown in figures 4 and 5, respectively. This fluid cannot be simulated using the conventional Gibbs ensemble because of the strength of the square-well bond. The simulations and theory agree well for both saturation densities and the fraction of monomers for $T^* < 1{\cdot}6$. However, the theory predicts a critical temperature that is significantly higher than that estimated from the simulations for this fluid. The theory appears to be inaccurate for calculating vapour–liquid equilibrium (VLE) near the critical point for strongly associating fluids. From figure 5 we see that there is considerable association in the vapour phase, and the fraction of monomers in the vapour phase increases with increasing temperature. This is in contrast to the results for moderately strong associating fluids [12] (see figure 3), where the fraction of monomers decreases monotonically as the critical temperature is approached. The difference between these two systems is a result of competing effects. Higher temperatures

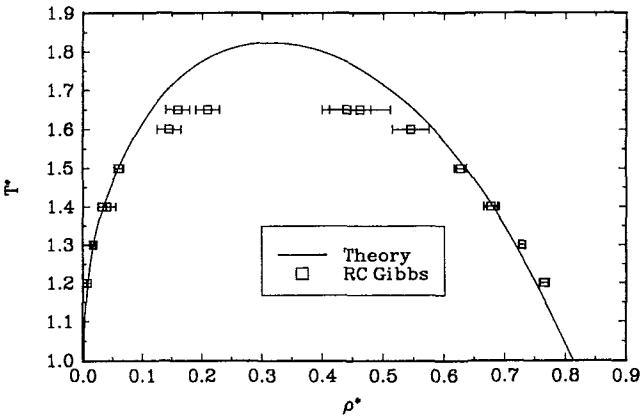

Figure 4. Saturation densities from reactive Gibbs ensemble simulations for a fluid with one square-well bonding site with $\epsilon^{bond} = 20\epsilon^{LJ}$. The line is calculated from the theory.

Downloaded by [Duke University Libraries] at 12:24 15 January 2013

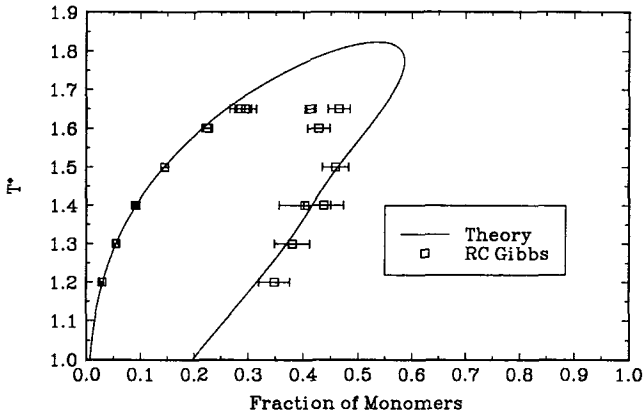

Figure 5. Fraction of monomers from reactive Gibbs ensemble simulations for a fluid with one square-well bonding site with $\epsilon^{\text{bond}} = 20\epsilon^{\text{LJ}}$. The line is calculated from the theory.

favour a higher fraction of monomers, but as the temperature increases the vapour phase density also increases, and higher densities favour a lower fraction of monomers. In the case of moderately strong bonding sites the density effects dominate, and the fraction of monomers decreases as the temperature increases. For the strongly bonding fluids studied here the temperature effects dominate at lower temperatures, giving an increasing fraction of monomers as the temperature increases. Near the critical temperature the situation is reversed and the fraction of monomers in the vapour phase decreases. Typical RC Gibbs ensemble runs were performed with 1000 molecules over several million configurations. The cut-off was taken at half the box length and standard long-range corrections were applied.

We have also performed RC Gibbs ensemble simulations for the simple association model of equations (16)–(18), using $D_0 = 25\epsilon^{\text{LJ}}$ and $r_e = \sigma$. The saturation densities are shown in figure 6 and the equilibrium fractions of monomers are shown in figure 7. The concentration of monomers in both the liquid and vapour phases is very low for this system, indicating that the RC Gibbs ensemble method is applicable

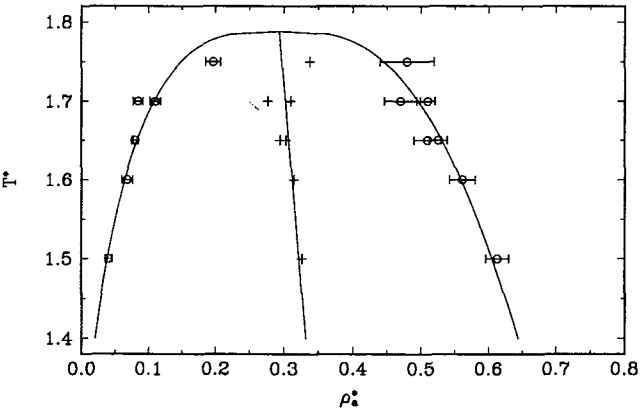

Figure 6. Simulation results from reactive Gibbs ensemble simulations for the reaction $2A \rightleftharpoons B$ with $D_0 = 25\epsilon^{\text{LJ}}$ and $r_e = \sigma$. The density ρ_a^* is the atomic number density. The lines are from the law of rectilinear diameters and the critical scaling law for the density.

Downloaded by [Duke University Libraries] at 12:24 15 January 2013

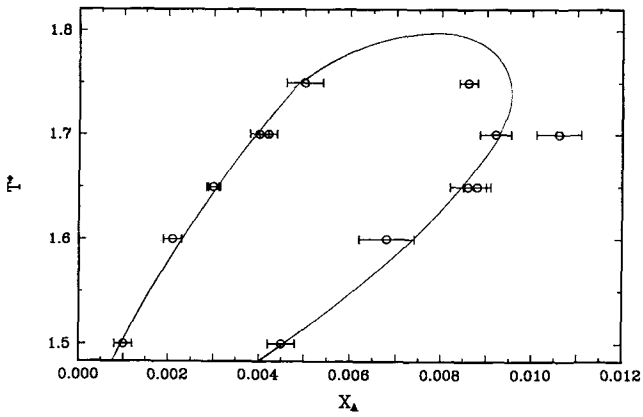

Figure 7. The fraction of type A molecules (monomers) for the reaction $2A \rightleftharpoons B$ from reactive Gibbs ensemble simulations. Intramolecular parameters are $D_0 = 25\epsilon^{LJ}$ and $r_e = \sigma$. X_A is the atomic fraction of monomers. The line is drawn as a guide to the eye.

to systems with very strong bonding. The system size used was $N = 512$, and the first 10^6 configurations were discarded for equilibration. Averages were collected for 10^6 to 2×10^6 configurations. Additional RC Gibbs simulations were performed for different values of D_0 and r_e in order to explore their effect on the critical temperature [26].

5. Comparison with experiment: nitric oxide dimerization

In this section we present results of RCMC simulations for liquid nitric oxide dimerization, and compare these results with experimental measurements of dissociation. It is well known that nitric oxide associates into dimers, but not higher aggregates due to its electronic structure. In addition, it is observed that nitric oxide is completely dimerized in the solid phase [27, 28], predominantly associated in the liquid phase at low temperatures [28, 29], and almost completely monomeric in the vapour phase at low pressures [27, 30]. Smith and Johnston [29] have used magnetic susceptibility measurements to calculate the fraction of monomers in liquid nitric oxide at several temperatures in the range $110\,K \leqslant T \leqslant 120\,K$. These measurements, coupled with the structural simplicity of the monomer, and the availability of structural and vibrational information for the monomer and dimer make nitric oxide an attractive system to study via computer simulations.

Following Kohler *et al.* [31], we have modelled nitric oxide as a single LJ sphere, and the dimer as a two-site LJ molecule. We have ignored the weak dipole moment of the monomer (0·2 D). In the RCMC simulations we have used the correct molecular partition functions for the monomer (two atoms) and the dimer (four atoms). Using a single LJ site for a diatomic molecule makes the model inconsistent. However, this is the same approach taken by Shaw [17], and is not expected to appreciably affect the results because the anisotropy of the NO molecule is relatively small. Note that the LJ potential need only account correctly for the average configurational energy, and not the details of the vibrations and rotations.

We have used $\epsilon/k = 125\,K$ and $\sigma = 3{\cdot}1715\,Å$ for the monomer LJ parameters as given by Kohler *et al.* [31]. The molecular constants for nitric oxide were taken from McQuarrie [32], and the electronic level information was taken from Reed and

Downloaded by [Duke University Libraries] at 12:24 15 January 2013

Downloaded by [Duke University Libraries] at 12:24 15 January 2013

Gubbins [33]. The parameters for the LJ site-site interactions for the dimer were the same as the monomer values. The bond length for the dimer was chosen as the N–N bond distance of 2·237 Å reported by Kukolich [34]. The dimer rotational constants were also taken from Kukolich [34], and the vibrational constants were taken from the work of Smith *et al.* [35]. The dissociation energy for the dimer can be calculated from the heat of formation of the dimer at a given temperature and the heat capacity for nitric oxide from that temperature to 0 K. Unfortunately, estimates for the heat of formation of $(NO)_2$ range from about 10 to 16 kJ mol^{-1} around 120 K, making the determination of the dissociation energy rather uncertain. We have used a value of 13·6 kJ mol^{-1}, which we obtained by adjusting the value of D_0 in short simulation runs at $T = 116$ K to achieve rough agreement between simulation and experiment for the fraction of monomers. Fortuitously, 13·6 kJ mol^{-1} is very close to the average of estimates by Smith and Johnston [29] (15·5 kJ mol^{-1}) and Guggenheim [30] (11·6 kJ mol^{-1}); this indicates that our potential model is at least reasonable.

No densities or pressures were given with the experimental values for the fraction of monomers. We therefore chose to perform our simulations in the RC *NPT* ensemble, specifying pressures close to the vapour pressures, which range from about 0·2 to 0·9 bar for the temperatures involved. The average reduced pressures from the simulations were close to zero. Simulations were initially carried out by starting with an initial configuration of 500 nitric oxide monomers. The site-site cut-off was 3σ, and the standard long-range corrections were applied. The system was typically equilibrated for 10^6 moves, followed by 4×10^6 moves for data taking. Some runs were started from previous configurations. The type of move attempted at a given step was decided at random with typical probabilities as follows: particle displacement/reorientation, 39%; association ($2NO \rightarrow (NO)_2$), 30%; dissociation ($(NO)_2 \rightarrow 2NO$), 30% volume move, 1%. Results of our simulations are plotted along with the experimental fraction of monomer data of Smith and Johnston [29] in figure 8. Agreement between simulation and experiment is excellent.

One might ask whether the agreement between simulation and experiment is due to adjusting the dissociation energy at 116 K. We have found that the simulations are sensitive to changes in the heat of formation of about 0·1 kJ mol^{-1} or more, and that

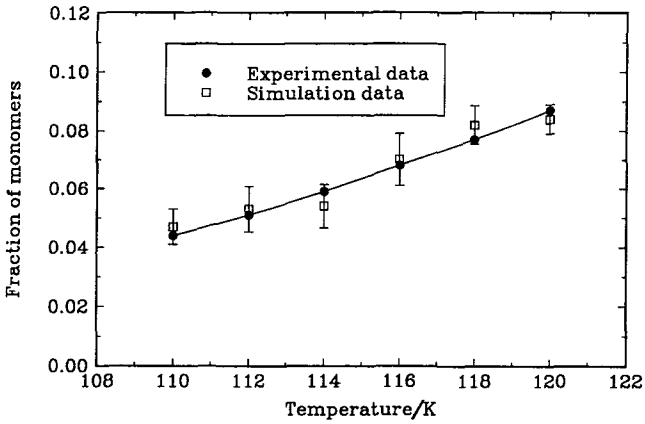

Figure 8. Fraction of monomers along the saturation line for liquid nitric oxide from RC *NPT* simulations and from the experiments of Smith and Johnston [29]. The line is drawn as a guide to the eye.

if the estimate of Smith and Johnston is used the simulations give fractions of monomers that are too small by about a factor of two. Hence, the simulations are quite sensitive to errors in the dissociation energy, and the limited temperature range covered by the experimental data does not pose a stringent test of our potential model. The sensitivity of the simulations to the value of the dissociation energy indicates that when there is substantial uncertainty in the value of the dissociation energy RCMC will not provide a reliable prediction of the extent of association or reaction. However, most dissociation energies are measured very accurately spectroscopically and in these cases RCMC should yield good predictions of equilibrium.

While we do not know of any other experimental measurements of the fraction of monomers in liquid nitric oxide, Guedes, [36] in connection with experimental studies of the thermodynamic properties of nitric oxide, has extrapolated the data of Smith and Johnston to higher temperatures. We have used these data as a further test of our simulation model. Guedes used the equilibrium constant and the heat of dissociation at 120 K from Smith and Johnston, and a value for the volume of dissociation at 116 K from Kohler *et al.* [31]. He assumed that both the heat and volume of dissociation were independent of temperature and pressure. With this information he extrapolated the fraction of monomers from 120 to 170 K at saturation pressures, which range from 0·9 to 43·3 bar. We have performed RC *NPT* ensemble simulations at the temperatures and saturation pressures Guedes reports, and these simulation results are compared to the extrapolated fractions of monomers in figure 9. The simulations agree with the extrapolated data up to 140 K, but for $T > 140$ K the simulations predict a higher fraction of monomers than the extrapolation. There are several possible causes of the discrepancy. The most obvious is that the heat of formation of the dimer is not a constant, as assumed by Guedes. Experimental data of Billingsley and Callear [37] for nitric oxide dimerization in the gas phase indicate that the heat of formation of the dimer decreases markedly above 140 K; this alone could account for the discrepancy. Other factors may include the use of an oversimplified pair potential, and temperature dependence of both the effective pair potential parameters and the volume of dissociation, although these latter effects are expected to be small.

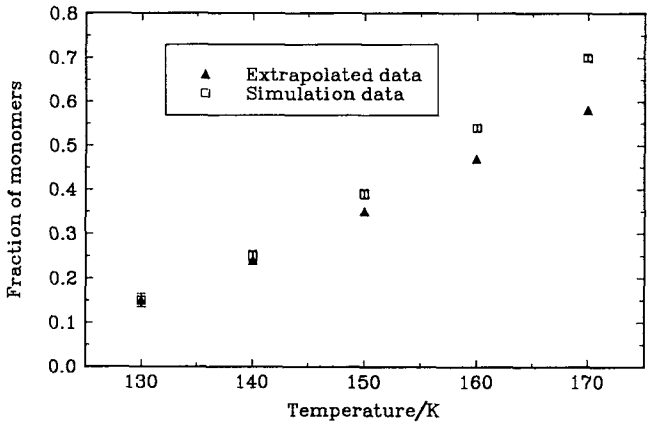

Figure 9. Fraction of monomers along the saturation line for liquid nitric oxide from RC *NPT* simulations and from an extrapolation of experimental data to higher temperatures and pressures [36].

Downloaded by [Duke University Libraries] at 12:24 15 January 2013

Nitric oxide is unusual in that dimerization in the vapour phase is remarkably low considering that the liquid is almost entirely dimerized at the normal boiling point. This contrasts with many other associating fluids. For example, acetic acid shows appreciable dimerization in both the liquid and vapour phases around its normal boiling point. Early estimates [27, 29, 35] indicated that dissociation of the nitric oxide dimer in the vapour was about 99% at the normal boiling point (121·4 K). Guggenheim [30] used the principle of corresponding states to analyse second virial coefficient data for nitric oxide, and calculated that the degree of dissociation in the saturated vapour is 98% at 121·4 K. We have performed a vapour phase RC *NPT* simulation at a pressure of 1·01 bar ($P^* = 0{\cdot}0019$) and $T = 121{\cdot}4$ K. The results of this simulation give the fraction of monomers as $0{\cdot}98 \pm 0{\cdot}0007$, in remarkable agreement with Guggenheim's estimate. By assuming ideal gas behaviour we calculate a density that is about 3% lower than the value from the simulation ($\rho^*_{\text{ideal}} = 1{\cdot}93 \times 10^{-3}$ while $\rho^*_{\text{sim}} = 1{\cdot}98 \times 10^{-3}$), but the fraction of monomers calculated from the ideal gas equilibrium constant is essentially the same as from the simulation.

6. Conclusions

We have developed a new simulation technique (RCMC) that facilitates the calculation of the properties of strongly associating fluids and chemically reacting mixtures. RCMC has also been implemented in conjunction with the isothermal–isobaric and Gibbs ensembles, in order to simultaneously calculate the phase and chemical equilibria of reactive mixtures.

The RCMC method has been tested by comparing with conventional grand canonical Monte Carlo simulations. Vapour–liquid phase equilibrium calculations for model associating fluids have been obtained from the reactive Gibbs ensemble. The temperature dependence of the fraction of monomers in the vapour phase for strongly associating fluids ($\epsilon^{\text{bond}} = 20\epsilon^{\text{LJ}}$) is qualitatively different from fluids with moderately strong bonding sites.

In contrast to the methods of Coker and Watts [13] and Kofke and Glandt [14], the RCMC method does not require the specification of chemical potential differences or fugacity fractions. The RCMC method does not constrain the values of the chemical potentials beyond the requirement of chemical equilibrium. No additional simulations are required to determine the properties of the system. Also, RCMC is applicable to reactions involving changes in the number of molecules.

We have compared experimental data for nitric oxide dimerization with RCMC simulations. Agreement for the fraction of monomers is excellent. Simulations at higher temperatures were compared to extrapolated data, and good agreement was found for temperatures below 140 K. For $T > 140$ K the simulations predict a higher fraction of monomers than does the extrapolation from experimental data. We have performed a vapour phase simulation at the normal boiling point and have found excellent agreement with estimates for dissociation in the vapour phase. Additional simulations for other chemical reactions are needed to verify the predictive capabilities of RCMC.

The RCMC technique has limitations. RCMC will fail at high fluid densities because monomers must successfully be inserted into the fluid. Cavity bias methods [38] or configurational bias methods [39–41] may be useful in extending the range of

Downloaded by [Duke University Libraries] at 12:24 15 January 2013

applicability. In practice, this method could become too cumbersome to implement for systems with many possible chemical reactions. Each species would need to be monitored and each reaction would need to be sampled with sufficient frequency to reach equilibrium and obtain accurate statistics. For some associating fluids the complement of possible reactions in unknown. Because of this it is unlikely that the RCMC method will be useful for treating associating fluids with multiple bonding sites, such as methanol and water.

It is a pleasure to thank R. Loring and M. S. Shaw for helpful discussions. J. K. J. acknowledges a National Research Council associateship at the Naval Research Laboratory. We thank the Gas Research Institute for support of this work under contract number 5091-260-2255.

Downloaded by [Duke University Libraries] at 12:24 15 January 2013

References

[1] WERTHEIM, M. S., 1984, *J. statist. Phys.*, **35,** 19.
[2] WERTHEIM, M. S., 1984, *J. statist. Phys.*, **35,** 35.
[3] WERTHEIM, M. S., 1986, *J. statist. Phys.*, **42,** 459.
[4] WERTHEIM, M. S., 1986, *J. statist. Phys.*, **42,** 477.
[5] WERTHEIM, M. S., 1986, *J. chem. Phys.*, **85,** 2929.
[6] WERTHEIM, M. S., 1987, *J. chem. Phys.*, **87,** 7323.
[7] WERTHEIM, M. S., 1988, *J. chem. Phys.*, **88,** 1145.
[8] JACKSON, G., CHAPMAN, W. G., and GUBBINS, K. E., 1988, *Molec. Phys.*, **65,** 1.
[9] STELL, G., and ZHOU, Y., 1989, *J. chem. Phys.*, **91,** 3618.
[10] ZHOU, Y., and STELL, G., 1992, *J. chem. Phys.*, **96,** 1504, 1507.
[11] CHAPMAN, W. G., 1990, *J. chem. Phys.*, **93,** 4299.
[12] JOHNSON, J. K., and GUBBINS, K. E., 1992, *Molec. Phys.*, **77,** 1033.
[13] COKER, D. F., and WATTS, R. O., 1981, *Chem. Phys. Lett.*, **78,** 333; *Molec. Phys.*, **44,** 1303.
[14] KOFKE, D. A., and GLANDT, E. D., 1988, *Molec. Phys.*, **64,** 1105.
[15] SINDZINGRE, P., CICCOTTI, G., MASSOBRIO, C., and FRENKEL, D., 1987, *Chem. Phys. Lett.*, **136,** 35.
[16] SINDZINGRE, P., MASSOBRIO, C., CICCOTTI, G., and FRENKEL, D., 1989, *Chem. Phys.*, **129,** 213.
[17] SHAW, M. S., 1991, *J. chem. Phys.*, **94,** 7550.
[18] PANAGIOTOPOULOS, A. Z., 1987, *Molec. Phys.*, **61,** 813.
[19] PANAGIOTOPOULOS, A. Z., QUIRKE, N., STAPLETON, M., and TILDESLEY, D. J., 1988, *Molec. Phys.*, **63,** 527.
[20] GRAY, C. C., and GUBBINS, K. E., 1984, *Theory of molecular fluids*, Vol. 1, chap. 3, (Oxford: Clarendon).
[21] ALLEN, M. P., and TILDESLEY, D. J., 1987, *Computer Simulation of Liquids* (Oxford: Clarendon).
[22] DENBIGH, K., 1966, *The Principles of Chemical Equilibrium* (Cambridge: Cambridge University Press).
[23] HILL, T. L., 1960, *An Introduction to Statistical Thermodynamics* (New York: Dover).
[24] WIDOM, B., 1963, *J. chem. Phys.*, **39,** 2808.
[25] WALSH, J., GUEDES, H. J. R., and GUBBINS, K. E., 1992, *J. phys. Chem.*, **96,** 10995.
[26] JOHNSON, J. K., 1992, Ph.D. Dissertation, Cornell University.
[27] JOHNSTON, H. L., and WEIMER, H. R., 1934, *J. Am. chem. Soc.*, **56,** 625.
[28] RICE, O. K., 1936, *J. chem. Phys.*, **4,** 367.
[29] SMITH, A. L., and JOHNSTON, H. L., 1952, *J. Am. chem. Soc.*, **74,** 4696.
[30] GUGGENHEIM, E. A., 1966, *Molec. Phys.*, **10,** 401; **11,** 403.
[31] KOHLER, F., BOHN, M., FISCHER, J., and ZIMMERMANN, R., 1987, *Monatshefte Chem.*, **118,** 169.

[32] McQuarrie, D. A., 1976, *Statistical Mechanics* (Harper & Row).
[33] Reed, T. M., and Gubbins, K. E., 1973, *Applied Statistical Mechanics* (McGraw-Hill), p. 92.
[34] Kukolich, S. G., 1982, *J. Am. chem. Soc.*, **104,** 4715.
[35] Smith, A. L., Keller, W. E., and Johnston, H. L., 1951, *J. chem. Phys.*, **19,** 189.
[36] Guedes, H. J. R., 1988, Ph.D. thesis, Universidade Nova de Lisboa, Portugal.
[37] Billingsley, J., and Callear, A. B., 1971, *Trans Faraday Soc.*, **67,** 589.
[38] Deitrick, G. L., Scriven, L. E., and Davis, H. T., 1989, *J. chem. Phys.*, **90,** 2370.
[39] dePablo, J. J., Laso, M., and Suter, U. W., 1992, *J. chem. Phys.*, **96,** 2395.
[40] dePablo, J. J., Laso, M., and Suter, U. W., 1992, *J. chem. Phys.*, **96,** 6157.
[41] Siepmann, J. I., and Frenkel, D., 1992, *Molec. Phys.*, **75,** 59.

Downloaded by [Duke University Libraries] at 12:24 15 January 2013